Magnesium isoglycyrrhizinate ameliorates doxorubicin-induced acute cardiac and hepatic toxicity via anti-oxidant and anti-apoptotic mechanisms in mice

ZHONGLIN WU[1], YUANYUAN ZHANG[2], TAO SONG[3], QIONGTAO SONG[3],
YING ZHANG[4], XUAN ZHANG[2], XUE HAN[2], JIANPING ZHANG[2] and LI CHU[2,3]

[1]Department of Radiology, The Fourth Hospital of Hebei Medical University, Shijiazhuang,
Hebei 050011; [2]Department of Pharmacology, Hebei University of Chinese Medicine, Shijiazhuang,
Hebei 050200; [3]Department of Pharmacology, Hebei Medical University, Shijiazhuang, Hebei 050017;
[4]Department of Pathology, Hebei University of Chinese Medicine, Shijiazhuang, Hebei 050200, P.R. China

Abstract. The present study investigated the effects and potential mechanisms of action of magnesium isoglycyrrhizinate (MgIG) in doxorubicin (DOX)-treated mice. Histopathological analysis and western blot analysis were conducted in the liver and heart tissues and biochemical analysis of the serum was performed. The results revealed that MgIG (10, 20 and 40 mg/kg/day) could protect the structure and functions of the liver and heart by inhibiting the activities of the myocardial enzymes creatine kinase (CK), CK-MB and lactate dehydrogenase and the hepatic-specific enzymes aspirate aminotransferase and alanine aminotransferase, increasing the activities of the antioxidants superoxide dismutase and glutathione peroxidase, and inhibiting cellular apoptosis induced by DOX (30 mg/kg). These results demonstrate that inhibiting lipid peroxidation and reducing myocardial and hepatocyte apoptosis may be one of the mechanisms by which MgIG exhibits hepatoprotective and cardioprotective effects in DOX-treated mice.

Introduction

Licorice root (*Glycyrrhiza uralensis Fisch*) is a traditional Chinese herbal medicine widely used in China and other Asian countries as a tonic herbal medicine, which is used to invigorate systems or promote general health (1). Glycyrrhizic acid is a water-soluble extract of the dried licorice rhizome that possesses anti-inflammatory,

anti-oxidative and liver-protective effects (2-4) and has two stereoisomers (18α and 18β). Magnesium isoglycyrrhizinate (MgIG) is a magnesium salt of 18α-glycyrrhizic acid, which exhibits important pharmacological activities. Previous studies have demonstrated that MgIG may inhibit inflammatory responses in through the phospholipase A_2/arachidonic acid and signal transducer and activator of transcription 3 pathways thus protecting liver function (5,6). Furthermore, MgIG protects liver cells from hypoxia-reoxygenation, ischemia/reperfusion and free fatty acid-induced injury (7-9). It has been suggested that MgIG exhibits potential hepatoprotective activity against hepatotoxicity induced by anticancer drugs (10). However, the effects and potential mechanisms of action of MgIG on the liver and heart remain unknown. Therefore, the current study aimed to identify the protective effects of MgIG on impairment in the liver and heart induced by doxorubicin (DOX).

DOX was introduced in the 1970s and has since become one of the most commonly used anthracycline antibiotics to treat hematological and solid tumors (11,12). However, even at clinically relevant doses, the therapeutic application of DOX is limited by systemic toxicity, including cardiotoxicity, hepatotoxicity and nephrotoxicity (13,14). DOX promotes reactive oxygen species (ROS), which mediates these organ toxicities (15-17). Cardiomyocytes are more vulnerable to attacks by oxygen free radicals since they are susceptible to ROS and contain lower levels of antioxidants, including glutathione peroxidase (GSH-Px) and superoxide dismutase (SOD) than other organs (16,18). The liver is another organ that is particularly sensitive to DOX, due to its metabolism and detoxification activities. It is estimated that ~40% of patients treated with DOX experience liver injury, since large amounts of DOX accumulate and are metabolized in the liver (15,19). Furthermore, the concurrent administration of DOX, paclitaxel and docetaxel enhances oxidative stress in the liver (20).

The present study investigated the effects and potential mechanisms of MgIG in DOX-treated mice to determine whether MgIG exhibits hepatoprotective and cardioprotective effects, in order to discern whether treatment with MgIG may

---

Correspondence to: Dr Li Chu, Department of Pharmacology, Hebei Medical University, 361 East Zhongshan Road, Shijiazhuang, Hebei 050017, P.R. China
E-mail: chuli0614@126.com

be an effective method of limiting the toxicity induced by DOX.

Materials and methods

Reagents. MgIG was supplied by Chia Tai Tianqing Pharmaceutical Group Co., Ltd. (Lianyungang, China; drug approval number, H20051942). DOX hydrochloride was purchased from Zhejiang Hisun Pharmaceutical Co. Ltd. (Zhejiang, China; drug approval number, H33021980).

Animals. A total of 50 male Kunming mice weighing 20.0 ± 2.0 g (4-5 weeks old) were purchased from the Laboratory Animal Center of Hebei Medical University (Shijiazhuang, China). The mice were housed in rust-free cages at 20-22°C and 45-55% relative humidity on a 12 h light-dark cycle, and given a normal pelleted diet and tap water *ad libitum*. All mice were handled according to the National Institutes of Health Guide for Care and Use of Laboratory Animals (21). All experiments were approved by the Ethics Committee for Animal Experiments of Hebei Medical University (approval number, HEBMU-2015-01; approval date, January 22, 2015).

Experimental design. Following a 1-week adaptation period, mice were randomly and divided into 5 equal groups (n=10/group): A control group [control, saline (normal saline 0.01 ml/g/day), intraperitoneal (i.p.)]; a model group (DOX, 30 mg/kg, i.p.); and treatment groups that received low-dose MgIG (L-MgIG, 10 mg/kg/day, i.p.), middle-dose MgIG (M-MgIG, 20 mg/kg/day, i.p.) and high-dose MgIG (H-MgIG, 40 mg/kg/day, i.p.). Mice in the treatment groups were administered MgIG for 1 week; then mice in the treatment and model groups were administered with 30 mg/kg DOX once. Following 48 h, all mice were weighed and anesthetized with sodium pentobarbital (50 mg/kg, i.p.). When the mice were anesthetized, blood was sampled from the eyes of the mice. The blood stood in the room temperature 30-60 min, and then the serum was separated (centrifuged at 2,200 x g for 10 min at room temperature) for biochemical analysis and liver and heart samples were quickly excised and snap frozen in liquid nitrogen or fixed in a 4% paraformaldehyde solution. The samples were then excised and examined as described below.

Histopathological analysis. Hepatic and cardiac tissue samples were fixed in 4% paraformaldehyde solution for ≥1 week at room temperature and embedded in paraffin. Paraffin-embedded samples were cut to 4-μm-thick sections, mounted on glass slides and stained with hematoxylin and eosin (H&E) for 50 min at room temperature for histopathological analysis, according to the conventional staining steps. To analyze the staining results, micrographs were scanned at x400 magnification with a digital light microscope (Leica DM750; Leica Microsystems GmbH, Wetzlar, Germany).

Serum biochemical analysis. Changes in the activity of the cardiac-specific enzymes creatine kinase (CK) (22), CK-MB and lactate dehydrogenase (LDH) in the serum were determined. Furthermore, levels of the two hepatic-specific enzymes aspartate aminotransferase (AST) (23) and alanine aminotransferase (ALT), the oxidative stress markers SOD and GSH-Px, and methane dicarboxylic aldehyde (MDA) were measured.

The activity of CK (cat. no. A032), CK-MB (cat. no. E006) and LDH (cat. no. A020-1) in the serum was determined at 37°C following the guidelines of the relevant assay kits (Nanjing Jiancheng Bioengineering Institute Co., Ltd., Nanjing, China). Serum levels of AST and ALT were detected by spectrophotometry-based methods following the guidelines of the AST (cat. no. C010-1) and ALT (cat. no. C009-1) assay kits (Nanjing Jiancheng Bioengineering Institute Co., Ltd.). SOD (cat. no. A001-1) and GSH-Px (cat. no. A005) activity, and MDA (cat. no. A003-1) serum levels were measured following the manuals of the corresponding assay kits (Nanjing Jiancheng Bioengineering Institute Co., Ltd.). All procedures were conducted in strict accordance with the manufacturer's protocols.

Western blot analysis. Total proteins were obtained from frozen liver and heart tissue homogenates following the manufacturer's protocol. The samples were homogenized and lysed with RIPA lysis buffer containing 50 mM Tris-HCl, 125 mM sodium chloride, 5 mM sodium pyrophosphate, 50 mM sodium fluoride, 1 mM EDTA, 1 mM dithiothreitol, 0.1% SDS (w/v), 1% TritonX-100 (v/v) and protease inhibitor cocktail (all Santa Cruz Biotechnology, Inc., Dallas, TX, USA). After incubation for 20 min on ice, the lysis buffer solution was centrifuged at 4°C at 7,800 x g for 20 min. The protein concentration was measured using a Bradford Protein Assay kit (Beyotime Institute of Biotechnology, Shanghai, China). ~50 μg of total proteins were loaded and separated on 10% SDS-PAGE, and then transferred to a nitrocellulose membrane. Membranes were blocked with blocking buffer (20 mM Tris-buffered saline and 0.1% Tween-20) containing 5% (w/v) non-fat milk for 2 h at room temperature and then incubated with the membrane was incubated with the primary antibody overnight at 4°C. The primary antibodies were are follows: Rabbit anti-caspase-3 (dilution 1:1,000; cat. no., sc-7148; Santa Cruz Biotechnology, Inc.), rabbit anti-B-cell lymphoma 2 (Bcl-2)-associated X protein (Bax; dilution 1:300; cat. no., BA0315; Wuhan Boster Biological Technology, Ltd., Wuhan, China), rabbit anti-Bcl-2 (dilution 1:1,000; cat. no., BS1031; Bioworld Technology, Inc., St. Louis Park, MN, USA), rabbit anti-nuclear factor (NF)-κBp65 (dilution 1:1,000; cat. no., BS1253; Bioworld Technology, Inc.) and mouse anti-β-actin (dilution 1:2,000; cat. no., TA-09; ZSGB-BIO; OriGene Technologies, Inc., Rockville, MD, USA) antibodies. Horseradish peroxidase conjugated goat anti-rabbit immunoglobulin (Ig)G (dilution 1:3,000; cat. no., ZB2305; ZSGB-BIO; OriGene Technologies, Inc.) or goat anti-mouse IgG (dilution, 1:3,000; cat. no., ZB2301; ZSGB-BIO; OriGene Technologies, Inc.) were used as the secondary antibodies. The membrane was incubated with the secondary antibodies at room temperature for 1 h. The bound antibodies were visualized using Amersham ECL Western Blotting Detection Reagent (GE Healthcare Life Sciences, Little Chalfont, UK) and quantified by densitometry using an image analyzer. The gray values of the hybridized bands were analyzed using Image-Pro Plus software (version 6.0; Media Cybernetics, Inc., Rockville, MD, USA). β-actin was used as an internal protein control for normalization.
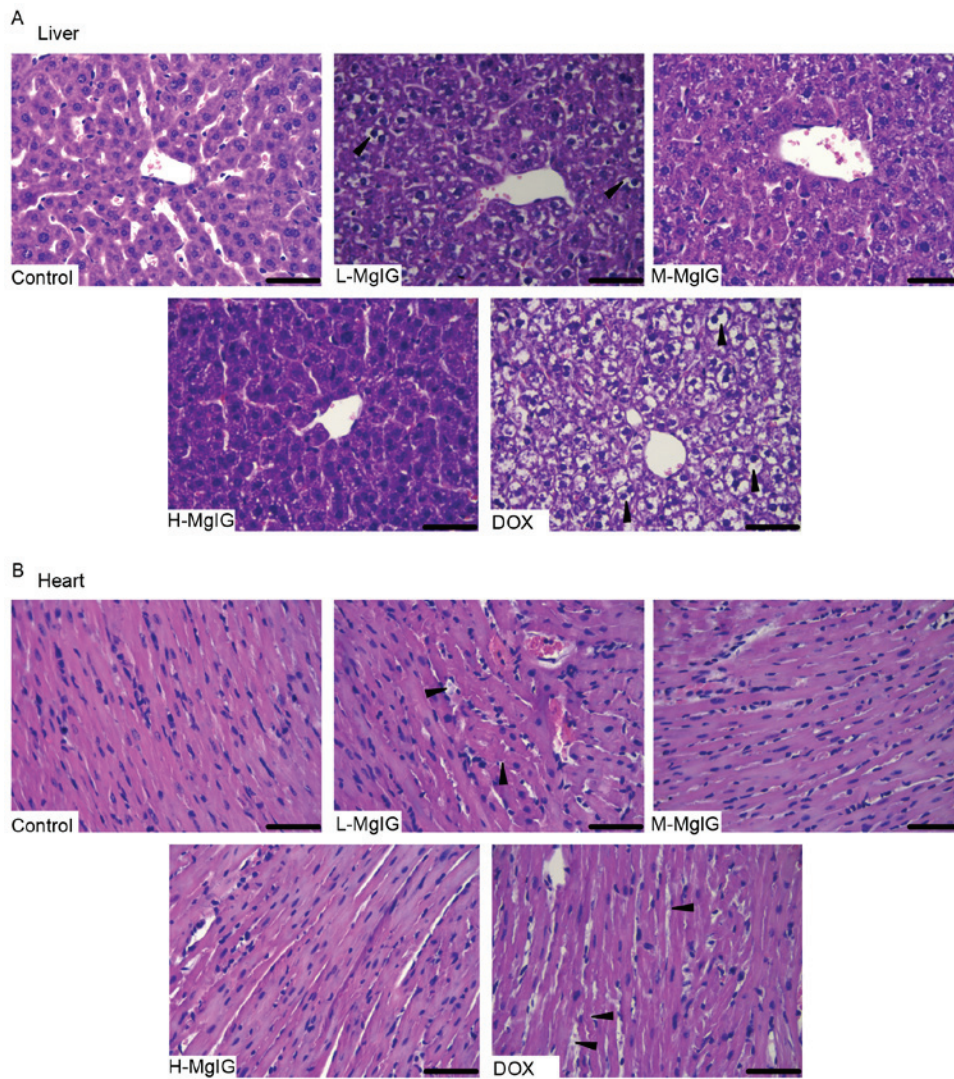
Figure 1. Effects of MgIG treatment on histological changes in (A) liver and (B) heart tissues induced by DOX. Representative morphological changes, indicated by black arrows, were stained with hematoxylin and eosin. Scale bar, 50 μm. Magnification, x400. MgIG, magnesium isoglycyrrhizinate; DOX, doxorubicin; L-MgIG, low-dose MgIG; M-MgIG, medium-dose MgIG; H-MgIG, high-dose MgIG.

Terminal deoxynucleotidyl transferase mediated dUTP nick end labeling (TUNEL) assay. TUNEL staining was performed using an *in situ* cell death detection kit (Roche Applied Science, Mannheim, Germany) following the manufacturer's protocol. Briefly, liver and the heart sections were deparaffinized, dehydrated using a series of increasing concentrations of alcohol, washed in distilled water followed by PBS and deproteinized using proteinase K (20 μg/ml) for 30 min at 37°C. Subsequently, sections were rinsed and incubated with the TUNEL reagent at 37°C for 1 h. Following rinsing, the sections were visualized using a peroxidase-conjugated anti-fluorescein antibody (in the TUNEL kit) with 0.02% 3,3-diaminobenzidine (Zhongshan Golden Bridge Biotechnology Co., Ltd., Beijing, China) and then counterstained with 0.5% hematoxylin at room temperature for 10-30 sec. Neutral balsam (Shanghai Guchen Biotechnology Co., Ltd., Shanghai, China) was used to bond the slides and cover glass together. To analyze the staining results, micrographs were scanned at x400 magnification with a digital light microscope system (Leica DM750). An image analysis system (Image-Pro Plus software; version 6.0) was used to analyze 20 randomly selected fields per slide at magnification x400 to determine the area of positive staining.

Data analysis. All data are provided as the mean ± standard error of the mean. Differences among the groups were assessed by one-way analysis of variance followed by Kruskal-Wallis and Tukey's tests. The statistical analysis software, Origin (version 7.5; OriginLab, Northampton, MA, USA) and SPSS (version 22.0; IBM Corp., Armonk, NY, USA) were used. $P<0.05$ was considered to indicate a statistically significant difference.

Results

Amelioration of morphological changes by MgIG. H&E staining was used to observe the histological changes of the liver and heart induced by DOX and the therapeutic effects of MgIG. Liver and heart tissue taken from the control group exhibited normal architecture (Fig. 1). However, in the DOX group, the hepatocytes became fatty, the nuclei were swollen and the liver cells dissolved due to putrescence, as indicated

Table I. Effects of MgIG injection on biochemical indexes changes in serum.

Groups	AST (IU/l)	ALT (IU/l)	CK (IU/l)	CK-MB (IU/l)	LDH (IU/l)
Control	121.79±6.24	56.68±2.45	494.01±18.37	208.55±9.78	300.90±13.14
L-MgIG	180.48±7.23[b]	94.49±3.69[b]	645.93±26.01[b]	298.37±11.92[b]	357.58±13.97[b]
M-MgIG	172.37±6.36[b]	87.78±3.44[b]	630.50±23.62[b]	296.63±9.98[b]	337.94±13.27[b]
H-MgIG	151.59±6.32[b]	79.64±2.42[b]	628.47±28.60[b]	268.44±12.39[b]	326.35±12.65[b]
DOX	258.61±9.85[a]	146.62±4.52[a]	894.92±31.65[a]	376.91±12.71[a]	512.81±16.23[a]

Data are presented as the mean ± standard error of the mean; [a]P<0.01 vs. control group; [b]P<0.01 vs. DOX group. AST, aspirate aminotransferase; ALT, alanine aminotransferase; CK, creatine kinase; LDH, lactate dehydrogenase; DOX, doxorubicin; MgIG, magnesium isoglycyrrhizinate; L-MgIG, low-dose MgIG; M-MgIG, medium-dose MgIG; H-MgIG, high-dose MgIG.

by the black triangles (Fig. 1A). Cardiomyocytes in the DOX group exhibited a disordered arrangement, breaks and necrosis, as indicated by the black triangles (Fig. 1B). However, in the MgIG pre-treatment groups, there was a decrease in the number of lesions in the liver and heart (Fig. 1A and B). These effects were greater in the medium-dose and high-dose MgIG groups.

Amelioration of biochemical index changes by MgIG. The changes in activity of the two hepatic-specific enzymes AST and ALT and the three cardiac-specific enzymes CK, CK-MB and LDH were measured in the serum to determine the protective effects of MgIG against DOX-induced damage in the liver and heart. As presented in Table I, AST and ALT activities in the DOX group (258.61±9.85 and 146.62±4.52 IU/l, respectively) increased ~2 to 3-fold compared with the control group (121.79±6.24 and 56.68±2.45 IU/l, respectively). However, serum ALT and AST activities in the MgIG pre-treatment groups were all significantly lower than in the DOX group (P<0.01). CK, CK-MB and LDH activity increased by ~2-fold in the DOX group compared with the control group. However, serum CK, CK-MB, and LDH activities in the MgIG pre-treatment groups were significantly lower than in the DOX group (P<0.01). The effects of MgIG in the liver and heart were dose-dependent, with greater decreases in serum ALT, AST, CK, CK-MB and LDH activity occurring in the groups treated with higher doses of MgIG.

Inhibition of oxidative stress by MgIG. Levels of the three oxidative stress markers SOD, GSH-Px and MDA in the serum were measured to assess the oxidative stress induced by DOX (Fig. 2). Compared with the control group, SOD and GSH-Px levels were significantly reduced (SOD: Control, 59.18±2.17 IU/mg vs. DOX, 26.18±1.14 IU/mg; GSH-Px: Control, 59.78±2.08 IU/mg vs. DOX, 31.39±1.94 IU/mg), whereas MDA levels were significantly increased in the DOX group (MDA: Control, 7.96±0.33 nmol/mg vs. DOX, 16.08±0.64 nmol/mg). However, pre-treatment with MgIG significantly increased SOD and GSH-Px and reduced MDA levels compared with the DOX group in a dose-dependent manner (P<0.01).

Suppression of apoptosis by MgIG. Levels of several apoptotic markers were measured by western blot analysis in the liver
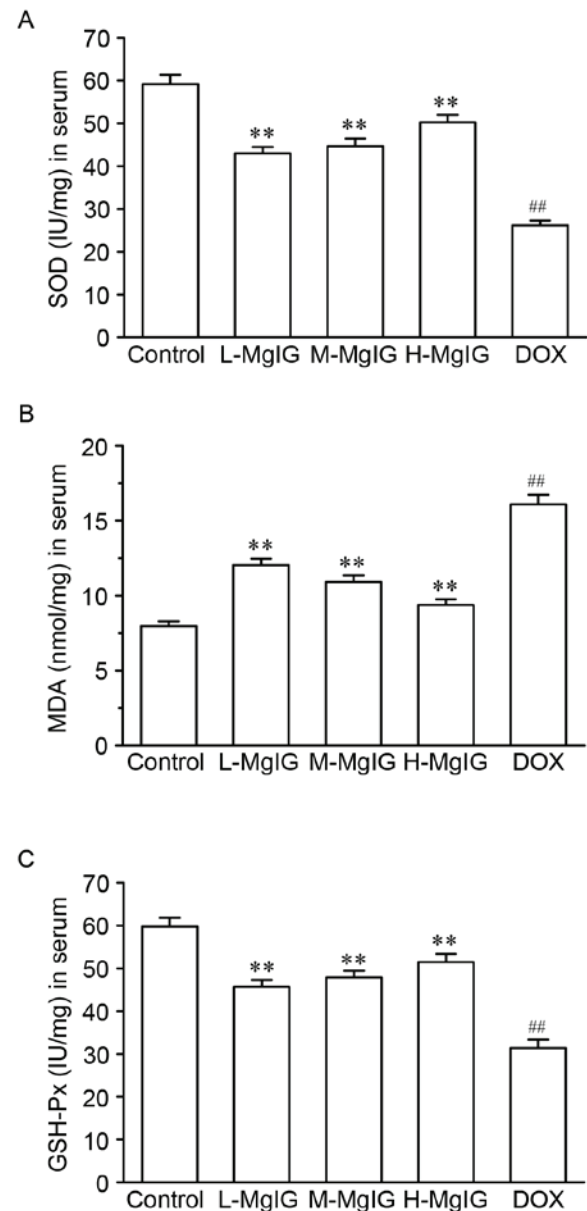

Figure 2. Effects of MgIG treatment on levels of oxidative stress parameters. The activities of (A) SOD, (B) MDA and (C) GSH-Px levels were measured in the serum. Data are presented the mean ± standard error of the mean. **P<0.01 vs. the DOX group; ##P<0.01 vs. the control group. MgIG, magnesium isoglycyrrhizinate; SOD, superoxide dismutase; GSH-Px, glutathione peroxidase; MDA, methane dicarboxylic aldehyde; DOX, doxorubicin; L-MgIG, low-dose MgIG; M-MgIG, medium-dose MgIG; H-MgIG, high-dose MgIG.
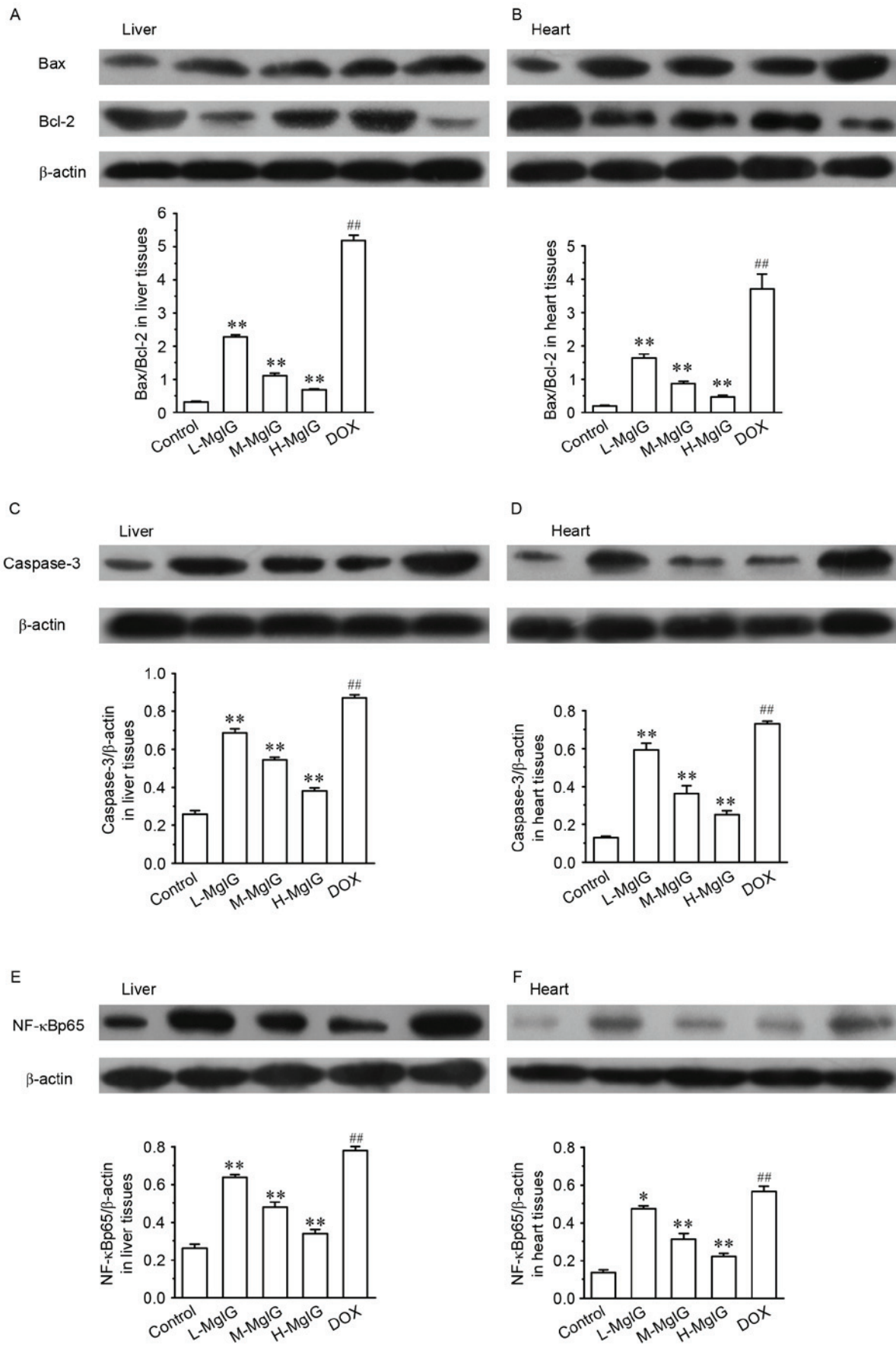
Figure 3. Effects of MgIG treatment on the expression of (A and B) Bax, Bcl-2, (C and D) caspase-3 and (E and F) NF-κBp65 in liver and heart tissues, measured by western blot analysis. The calculated relative intensities of Bax/Bcl-2, caspase-3/β-actin, and NF-κBp65/β-actin are presented under the representative immunoblots for each group. Data are presented the mean ± standard error of the mean. *P<0.05 and **P<0.01 vs. the DOX group; ##P<0.01 vs. the control group. MgIG, magnesium isoglycyrrhizinate; Bcl-2, B-cell lymphoma 2; Bax, Bcl-2-associated X protein; NF-κBp65, nuclear factor κBp65; DOX, doxorubicin; L-MgIG, low-dose MgIG; M-MgIG, medium-dose MgIG; H-MgIG, high-dose MgIG.
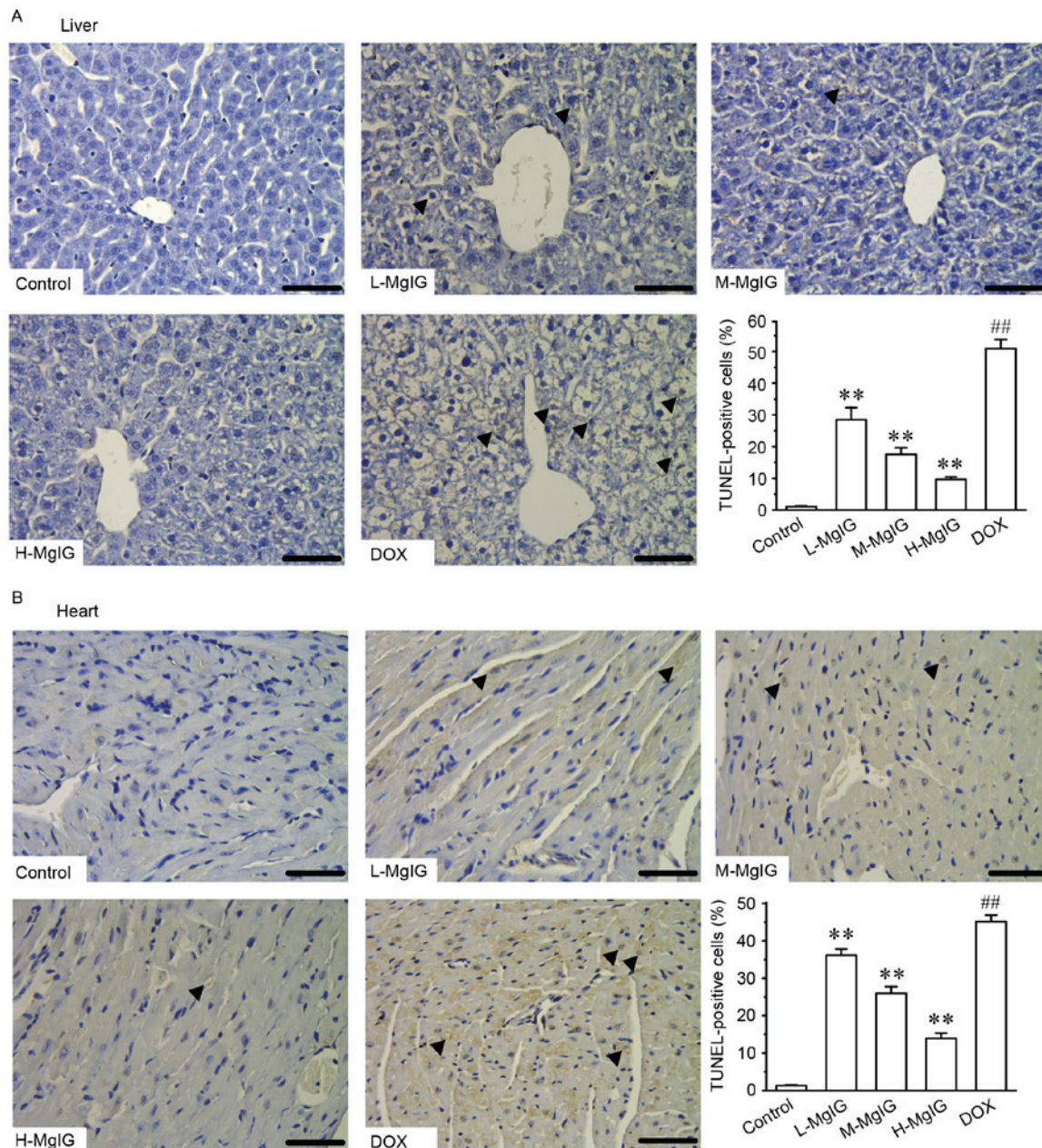
Figure 4. Effects of MgIG treatment on apoptosis detected by TUNEL staining in (A) liver and (B) heart tissues. Representative images of apoptotic cells (marked by black arrows) and graphs of the proportion of positive cells in each group are presented. Scale bar=50 μm; magnification, x400. Data are presented the mean ± standard error of the mean. **P<0.01 vs. the DOX group; ##P<0.01 vs. the control group. MgIG, magnesium isoglycyrrhizinate; TUNEL, terminal deoxynucleotidyl transferase dUTP nick end labeling; DOX, doxorubicin; L-MgIG, low-dose MgIG; M-MgIG, medium-dose MgIG; H-MgIG, high-dose MgIG.

and heart tissues (Fig. 3). Compared with the control group, the expression of Bax/Bcl-2, caspase-3 and NF-κBp65 were significantly upregulated in the DOX groups (all P<0.01). However, in the MgIG pre-treatment groups, the expression of Bax/Bcl-2, caspase-3 and NF-κBp65 were significantly reduced in a dose-dependent manner compared with the DOX group (all P<0.01). This indicates that MgIG treatment increases the anti-apoptotic abilities of hepatocytes and cardiomyocytes.

Additionally, TUNEL staining was used to assess apoptosis in cardiac and hepatic cells. Apoptosis in hepatic and cardiac cells remained at consistently low levels in the control group (Fig. 4). However, the number of TUNEL-positive cardiac and

hepatic cells was significantly increased in the DOX group compared with the control group (P<0.01). However, treatment with MgIG significantly decreased the extent of apoptosis compared with the DOX group in a dose-dependent manner (P<0.01).

Discussion

Licorice is described in one of the oldest *materia medica* texts, 'Shennong's Classic Materia Medica' and has been used to treat various ailments in China for centuries due to its beneficial properties (24). Glycyrrhizic acid is one of its primary active components and exhibits antiviral and antimicrobial

activities (24). As an important stereoisomer of glycyrrhizic acid, MgIG is commonly used as a hepatoprotective medicine, which induces fewer side-effects than other similar treatments (25). Furthermore, it has been demonstrated that MgIG exhibits hepatoprotective activity against the hepatotoxicity induced by anticancer drugs (10), in a liver injury model induced by hepatectomy (6) and in a hypoxia/reoxygenation injury (ischemia/reperfusion) model in liver cells (8). The results of the present indicated that MgIG exhibits hepato- and cardioprotective effects. The results of H&E staining obtained from liver and heart tissues demonstrate that the extent of injuries induced by DOX was decreased in mice that received MgIG pre-treatment, indicating that MgIG exhibits hepato- and cardioprotective effects.

Transaminase is an indicator of liver function and is indispensable as a catalyst in the process of human metabolism. The serum levels of AST and ALT increase rapidly when liver cells are damaged by inflammation, necrosis or poisoning (26). It was demonstrated that serum levels of AST and ALT in the MgIG-treatment groups were significantly lower than in the DOX group, indicating that MgIG exerts its protective effects in the liver by regulating the activity of AST and ALT. To examine the cardioprotective effects, the serum levels of CK, CK-MB and LDH, which are usually used in the evaluation of myocardial injury (27-29), were measured in the present study. MgIG reversed the increase in the activities of myocardial enzymes induced by DOX. This indicates that MgIG may ameliorate heart injury by regulating the activity of AST and ALT.

Over the past few decades, the number of cancer cases has increased. More patients require treatment for cancer and experience severe side-effects following treatment with various anti-cancer drugs (30,31). DOX is used clinically as an anti-cancer drug, however its therapeutic application is been limited due to the serious adverse reactions experienced by patients, which affect the heart, liver and other organs (13,14). In the current study, a high dose of DOX was used to induce cardiotoxicity and hepatotoxicity in mice. The results revealed that MgIG may, at least in part, alleviate the acute toxicity induced by DOX. Its underlying mechanism of action may be associated with the antioxidant stress and the anti-apoptotic activities of MgIG.

Following acute stimulus with high doses of DOX, the body may generate excessive free radicals, thus triggering massive peroxidation and resulting in antioxidant depletion (32-34). SOD and GSH-Px belong to the ROS scavenger enzymatic system and may neutralize certain reactive molecules and counterbalance the oxidative destruction induced by free radicals (35,36). MDA is a representative aldehydic lipid peroxidative product that is poisonous to cells (37). The present study indicated that serum levels of SOD and GSH-Px were reduced and that concentrations of MDA were elevated in DOX-treated mice, demonstrating that peroxidation was induced by DOX. In all groups receiving treatment with MgIG, SOD and GSH-Px levels increased, whereas those of MDA decreased. The results of previous studies indicated that oxidative stress is responsible for the cardiotoxicity and hepatotoxicity induced by DOX and is associated with decreased activity of the antioxidant system (20,38,39). As a consequence, it was hypothesized that MgIG may improve the body's antioxidant capacity, which may be an important

mechanism of MgIG in resisting damage to the liver and heart induced by DOX.

Elevated ROS may induce apoptotic cell death and damage to tissues and organs (40-42). NF-κBp65 is predominant in the apoptotic regulation process by regulating the expression of downstream Bcl-2 genes. Bax participates in apoptotic responses via intrinsic mitochondrial-dependent signaling by inducing the release of cytochrome c (23,43-45). Another cell death protease is caspase-3, which serves a role in cell apoptosis. The activation of apoptotic pathways finally results in the activation of caspase-3 (46). In the present study, the expression of Bax/Bcl-2, caspase-3 and NF-κBp65 were all significantly increased in liver and heart tissues of the group exposed to DOX. These observations reveal that exposure to high-doses of DOX enhances apoptosis. However, treatment with MgIG significantly reduced expression of the apoptotic factors Bax/Bcl-2, caspase-3 and NF-κBp65 and decreased the number of TUNEL-positive cells in the liver and heart tissues. Furthermore, the effects of MgIG in the high-dose group were greater compared with the other groups, indicating that MgIG acts in a dose-dependent manner. This may be another important molecular mechanism by which MgIG protects against the hepatotoxicity and cardiotoxicity induced by DOX.

In conclusion, the results of the present study demonstrate that MgIG may help to ameliorate DOX-induced liver and heart injuries in mice. One of its mechanisms of action may be its anti-lipid peroxidation and anti-apoptotic effects in hepatocytes and cardiomyocytes. These observations indicate that MgIG may be used as a novel treatment to protect the liver and heart from adverse reactions induced by anti-cancer drugs.

Acknowledgements

References

1. Andersen-Parrado P: Licorice: Not just candy, but a tonic herb with myriad healing properties. Better Nutrition 59: 33-34, 1997.
2. Cosmetic Ingredient Review Expert Panel: Final report on the safety assessment of glycyrrhetinic acid, potassium glycyrrhetinate, disodium succinoyl glycyrrhetinate, glyceryl glycyrrhetinate, glycyrrhetinyl stearate, stearyl glycyrrhetinate, glycyrrhizic acid, ammonium glycyrrhizate, dipotassium glycyrrhizate, disodium glycyrrhizate, trisodium glycyrrhizate, methyl glycyrrhizate, and potassium glycyrrhizinate. Int J Toxicol 26 (Suppl 2): S79-S112, 2007.
3. Ming LJ and Yin AC: Therapeutic effects of glycyrrhizic acid. Nat Prod Commun 8: 415-418, 2013.
4. van Rossum TG, Vulto AG, de Man RA, Brouwer JT and Schalm SW: Review article: Glycyrrhizin as a potential treatment for chronic hepatitis C. Aliment Pharmacol Ther 12: 199-205, 1998.
5. Xie C, Li X, Wu J, Liang Z, Deng F, Xie W, Zhu M, Zhu J, Zhu W, Geng S, et al: Anti-inflammatory activity of magnesium isoglycyrrhizinate through inhibition of phospholipase a2/arachidonic acid pathway. Inflammation 38: 1639-1648, 2015.
6. Tang GH, Yang HY, Zhang JC, Ren JJ, Sang XT, Lu X, Zhong SX and Mao YL: Magnesium isoglycyrrhizinate inhibits inflammatory response through STAT3 pathway to protect remnant liver function. World J Gastroenterol 21: 12370-12380, 2015.

7. Zheng J, Wu G, Hu GX, Peng YZ and Xiong XJ: Protective effects against and potential mechanisms underlying the effect of magnesium isoglycyrrhizinate in hypoxia-reoxygenation injury in rat liver cells. Genet Mol Res 14: 15453-15461, 2015.

8. Huang X, Qin J and Lu S: Magnesium isoglycyrrhizinate protects hepatic L02 cells from ischemia/reperfusion induced injury. Int J Clin Exp Pathol 7: 4755-4764, 2014.

9. Cheng Y, Zhang J, Shang J and Zhang L: Prevention of free fatty acid-induced hepatic lipotoxicity in HepG2 cells by magnesium isoglycyrrhizinate in vitro. Pharmacology 84: 183-190, 2009.

10. Vincenzi B, Armento G, Spalato Ceruso M, Catania G, Leakos M, Santini D, Minotti G and Tonini G: Drug-induced hepatotoxicity in cancer patients-implication for treatment. Expert Opin Drug Saf 15: 1219-1238, 2016.

11. Kalyanaraman B: Teaching the basics of redox biology to medical and graduate students: Oxidants, antioxidants and disease mechanisms. Redox Biol 1: 244-257, 2013.

12. Aleisa AM, Al-Rejaie SS, Bakheet SA, Al-Bekari AM, Al-Shabanah OA, Al-Majed A, Al-Yahya AA and Qureshi S: Effect of metformin on clastogenic and biochemical changes induced by adriamycin in Swiss albino mice. Mutat Res 634: 93-100, 2007.

13. Panda S and Kar A: Periplogenin-3-O- -D-glucopyranosyl -(1->6)- -D-glucopyaranosyl- -(1->4) -D-cymaropyranoside, isolated from Aegle marmelos protects doxorubicin induced cardiovascular problems and hepatotoxicity in rats. Cardiovasc Ther 27: 108-116, 2009.

14. Zordoky BN, Anwar-Mohamed A, Aboutabl ME and El-Kadi AO: Acute doxorubicin toxicity differentially alters cytochrome P450 expression and arachidonic acid metabolism in rat kidney and liver. Drug Metab Dispos 39: 1440-1450, 2011.

15. Wang Y, Mei X, Yuan J, Lu W, Li B and Xu D: Taurine zinc solid dispersions attenuate doxorubicin-induced hepatotoxicity and cardiotoxicity in rats. Toxicol Appl Pharmacol 289: 1-11, 2015.

16. Dong Q, Chen L, Lu Q, Sharma S, Li L, Morimoto S and Wang G: Quercetin attenuates doxorubicin cardiotoxicity by modulating Bmi-1 expression. Br J Pharmacol 171: 4440-4454, 2014.

17. Indu R, Azhar TS, Nair A and Nair CK: Amelioration of doxorubicin induced cardio-and hepato-toxicity by carotenoids. J Cancer Res Ther 10: 62-67, 2014.

18. Kalyanaraman B, Joseph J, Kalivendi S, Wang S, Konorev E and Kotamraju S: Doxorubicin-induced apoptosis: Implications in cardiotoxicity. Mol Cell Biochem 234-235: 119-124, 2002.

19. Tacar O, Sriamornsak P and Dass CR: Doxorubicin: An update on anticancer molecular action, toxicity and novel drug delivery systems. J Pharm Pharmacol 65: 157-170, 2013.

20. Pieniazek A, Czepas J, Piasecka-Zelga J, Gwoździński K and Koceva-Chyła A: Oxidative stress induced in rat liver by anticancer drugs doxorubicin, paclitaxel and docetaxel. Adv Med Sci 58: 104-111, 2013.

21. National Institute of Health: Guide for the Care and Use of Laboratory Animals. The National Academies Press, Washington, DC, 1996.

22. Arola OJ, Saraste A, Pulkki K, Kallajoki M, Parvinen M and Voipio-Pulkki LM: Acute doxorubicin cardiotoxicity involves cardiomyocyte apoptosis. Cancer Res 60: 1789-1792, 2000.

23. Wang L, Yang R, Yuan B, Liu Y and Liu C: The antiviral and antimicrobial activities of licorice, a widely-used Chinese herb. Acta Pharm Sin B 5: 310-315, 2015.

24. Yang Q, Wang J, Liu R, Wang Z, Li Y, Zhang Y, Hao X, Huang Y, Xie W and Wei H: Amelioration of concanavalin A-induced autoimmune hepatitis by magnesium isoglycyrrhizinate through inhibition of CD4(+)CD25(-)CD69(+) subset proliferation. Drug Des Devel Ther 10: 443-453, 2016.

25. Navarro VJ and Senior JR: Drug-related hepatotoxicity. N Engl J Med 354: 731-739, 2006.

26. Zhang JP, Zhang YY, Zhang Y, Gao YG, Ma JJ, Wang N, Wang JY, Xie Y, Zhang FH and Chu L: Salvia miltiorrhiza (Danshen) injection ameliorates iron overload-induced cardiac damage in mice. Planta Med 79: 744-752, 2013.

27. Dawson EA, Shave R, George K, Whyte G, Ball D, Gaze D and Collinson P: Cardiac drift during prolonged exercise with echocardiographic evidence of reduced diastolic function of the heart. Eur J Appl Physiol 94: 305-309, 2005.

28. Chan EM, Thomas MJ, Bandy B and Tibbits GF: Effects of doxorubicin, 4'-epirubicin, and antioxidant enzymes on the contractility of isolated cardiomyocytes. Can J Physiol Pharmacol 74: 904-910, 1996.

29. Shirakami Y, Sakai H and Shimizu M: Retinoid roles in blocking hepatocellular carcinoma. Hepatobiliary Surg Nutr 4: 222-228, 2015.

30. Shrum B, Costello P, McDonald W, Howlett C, Donnelly M and McAlister VC: In vitro three dimensional culture of hepatocellular carcinoma to measure prognosis and responsiveness to chemotherapeutic agents. Hepatobiliary Surg Nutr 5: 204-208, 2016.

31. González-Vallinas M and Breuhahn K: MicroRNAs are key regulators of hepatocellular carcinoma (HCC) cell dissemination-what we learned from microRNA-494. Hepatobiliary Surg Nutr 5: 372-376, 2016.

32. Ozben T: Oxidative stress and apoptosis: Impact on cancer therapy. J Pharm Sci 96: 2181-2196, 2007.

33. Conklin KA: Chemotherapy-associated oxidative stress: Impact on chemotherapeutic effectiveness. Integr Cancer Ther 3: 294-300, 2004.

34. Zhang Y, Wang H, Cui L, Zhang Y, Liu Y, Chu X, Liu Z, Zhang J and Chu L: Continuing treatment with Salvia miltiorrhiza injection attenuates myocardial fibrosis in chronic iron-overloaded mice. PLoS One 10: e0124061, 2015.

35. Fridovich I: Oxygen radicals from acetaldehyde. Free Radic Biol Med 7: 557-558, 1989.

36. Forman HJ and Dickinson DA: Introduction to serial reviews on 4-hydroxy-2-nonenal as a signaling molecule. Free Radic Biol Med 37: 594-596, 2004.

37. Gutteridge JM: Lipid peroxidation and antioxidants as biomarkers of tissue damage. Clin Chem 41: 1819-1828, 1995.

38. Zhou S, Palmeira CM and Wallace KB: Doxorubicin-induced persistent oxidative stress to cardiac myocytes. Toxicol Lett 121: 151-157, 2001.

39. Kalender Y, Yel M and Kalender S: Doxorubicin hepatotoxicity and hepatic free radical metabolism in rats. The effects of vitamin E and catechin. Toxicology 209: 39-45, 2005.

40. Robinson P, Kasembeli M, Bharadwaj U, Engineer N, Eckols KT and Tweardy DJ: Substance P receptor signaling mediates doxorubicin-induced cardiomyocyte apoptosis and triple-negative breast cancer chemoresistance. Biomed Res Int 2016: 1959270, 2016.

41. Krishnamurthy B, Rani N, Bharti S, Golechha M, Bhatia J, Nag TC, Ray R, Arava S and Arya DS: Febuxostat ameliorates doxorubicin-induced cardiotoxicity in rats. Chem Biol Interact 237: 96-103, 2015.

42. Zhang YW, Shi J, Li YJ and Wei L: Cardiomyocyte death in doxorubicin-induced cardiotoxicity. Arch Immunol Ther Exp (Warsz) 57: 435-445, 2009.

43. Beere HM, Wolf BB, Cain K, Mosser DD, Mahboubi A, Kuwana T, Tailor P, Morimoto RI, Cohen GM and Green DR: Heat-shock protein 70 inhibits apoptosis by preventing recruitment of procaspase-9 to the Apaf-1 apoptosome. Nat Cell Biol 2: 469-475, 2000.

44. Zheng B, Wu L, Ma L, Liu S, Li L, Xie W and Li X: Telekin induces apoptosis associated with the mitochondria-mediated pathway in human hepatocellular carcinoma cells. Biol Pharm Bull 36: 1118-1125, 2013.

45. Nagai K, Oda A and Konishi H: Theanine prevents doxorubicin-induced acute hepatotoxicity by reducing intrinsic apoptotic response. Food Chem Toxicol 78: 147-152, 2015.

46. Muller I, Niethammer D and Bruchelt G: Anthracycline-derived chemotherapeutics in apoptosis and free radical cytotoxicity (Review). Int J Mol Med 1: 491-494, 1998.